Soft Matter

PAPER

Cite this: *Soft Matter*, 2018, **14**, 3563

Fatigue fracture of nearly elastic hydrogels

Enrui Zhang,† Ruobing Bai,† Xavier P. Morelle and Zhigang Suo *

Received 6th March 2018,
Accepted 16th April 2018

DOI: 10.1039/c8sm00460a

rsc.li/soft-matter-journal

Polyacrylamide hydrogels are highly stretchable and nearly elastic. Their stress–stretch curves exhibit small hysteresis, and change negligibly after many loading cycles. Polyacrylamide is used extensively in applications, and is the primary network for many types of tough hydrogels. Recent experiments have shown that polyacrylamide hydrogels are susceptible to fatigue fracture, but available data are limited. Here we study fatigue fracture of polyacrylamide hydrogels of various water contents. We form polymer networks in all samples under the same conditions, and then obtain hydrogels of 96, 87, 78, and 69 wt% of water by solvent exchange. We measure the crack extension under cyclic loads, and the fracture energy under monotonic loading. For the hydrogels of the four water contents, the fatigue thresholds are 4.3, 8.4, 20.5, and 64.5 J m^{-2}, and the fracture energies are 18.9, 71.2, 289, and 611 J m^{-2}. The measured thresholds agree well with the predictions of the Lake-Thomas model for hydrogels of high water content, but not in the case of low water content. It is hoped that further basic studies will soon follow to aid the development of fatigue-resistant hydrogels.

1. Introduction

Since the landmark paper by Wichterle and Lim,[1] in 1960, synthetic hydrogels have developed into a class of materials of their own, principally for personal care and medical applications, such as contact lenses,[2] superabsorbent diapers,[3] tissue engineering,[4,5] drug delivery,[6,7] wound dressing,[8] and artificial tissues.[9,10] In recent years, hydrogels have also been used to develop nonmedical applications. Examples include artificial muscles,[11–20] artificial skins,[21–27] artificial axons,[28] artificial eels,[29] optical fibers,[30–32] fire-retarding blankets,[33] touchpads,[34] triboelectric generators,[35–37] liquid crystal devices,[38] and ionotronic luminescent devices.[39,40] Hydrogels are highly stretchable, transparent, ionic conductors.[11] Hydrogels can retain water in the open air when hydrogels dissolve hygroscopic salts[41] and are coated with hydrophobic elastomers.[22,25,42] Hydrogels containing salts can remain soft at temperatures below 0 °C.[41] Hydrogels coated with elastomers can sustain temperatures above 100 °C without boiling.[43] The property space further spans extensively when hydrogels are integrated with other materials to form water matrix composites (WMC).[10,44–47] Also under development are methods to create strong adhesion between hydrophilic and hydrophobic polymer networks,[24,25,43,48] and methods to fabricate integrated hydrogel devices through casting, coating, and printing.[20,23,49–51]

Of particular relevance to this paper is the discovery of hydrogels of extraordinary toughness.[52] Most hydrogels are fragile, like tofu and Jell-O. A polyacrylamide hydrogel can be stretched several times its original length, but ruptures at a small stretch when the sample is pre-cut with a crack of length exceeding a few millimeters. This flaw sensitivity is common to all materials, but different materials are sensitive to flaws of different sizes.[53,54] Flaw sensitivity is inversely related to a material property: fracture energy (also called toughness).[53] The toughness is about 1–10 J m^{-2} for tofu and Jell-O, about 100 J m^{-2} for polyacrylamide hydrogels, about 1000 J m^{-2} for cartilage, and above 10 000 J m^{-2} for natural rubber. Hydrogels as tough as natural rubber have been developed.[9,52,55–63] A tough hydrogel has a stretchable polymer network in topological entanglement with a network with sacrificial bonds. The hydrogel is tough when the stretchable polymer network is strong enough to break the sacrificial bonds in a large volume surrounding the front of a crack. That is, the sacrificial bonds act as tougheners. The discovery of this fundamental principle has instigated the worldwide search for hydrogels of various polymer networks and sacrificial bonds,[9,52,55–63] and for applications of hydrogels previously unimagined.[7–9,18,63]

Like all materials, as the property space spans and applications proliferate, hydrogels will be pushed into uses under extreme conditions. In particular, many applications will require hydrogels to sustain cyclic mechanical loads. For example, hydrogels will sustain cyclic deformation in artificial tissues,[10] move repeatedly in soft robotic arms,[12–19] stretch and relax in artificial skins,[21–27] and vibrate in transparent loudspeakers.[11] Fatigue fracture has been studied exhaustively in all established

John A. Paulson School of Engineering and Applied Sciences, Kavli Institute for Bionano Science and Technology, Harvard University, Cambridge, MA 02138, USA. E-mail: suo@seas.harvard.edu

† These authors contributed equally to this work.

load-bearing materials, including metals, ceramics, plastics, elastomers, and composites.[64–72] A steel, for example, can survive an unlimited number of cycles if the amplitude of load is below an endurance limit.[72] However, if the steel contains a large enough crack, the crack will extend cycle by cycle. To enable new applications of hydrogels, as well as to aid the further development of hydrogels, it is urgent to study fatigue fracture of hydrogels.

We have recently initiated the study of fatigue fracture of hydrogels.[73–76] To explore principles that might aid the development of fatigue-resistant hydrogels, we have focused our study on the chemistry of fatigue. Hydrogels studied for fatigue fracture so far all contain at least a covalent network of polyacrylamide. Fatigue fracture has been observed in all of them, including polyacrylamide hydrogels,[73] alginate–polyacrylamide hydrogels in which alginate is ionically crosslinked,[74] poly(2-acrylamido-2-methylpropane sulfonic acid)–polyacrylamide hydrogels in which PAMPS forms a short-chain covalent network,[75] and poly(vinyl alcohol)–polyacrylamide hydrogels in which PVA provides reversible, noncovalent interactions.[76] For all the hydrogels studied so far, the threshold for fatigue fracture, below which the crack does not propagate under cyclic loads, is considerably lower than the toughness measured under monotonic loading. The threshold depends on the long-chain covalent networks (*i.e.*, the polyacrylamide networks for hydrogels studied so far), but negligibly on the toughheners. When the hydrogels are subject to cyclic loads above the threshold, the toughheners do markedly reduce the extension of crack per cycle.

This paper focuses on fatigue fracture of polyacrylamide (PAAm) hydrogels. A PAAm hydrogel contains a covalent network, but negligible toughheners. As a result, PAAm hydrogels are highly stretchable and nearly elastic.[73,74,77,78] The stress–stretch curves exhibit little hysteresis, and change negligibly after thousands of cycles of loads.[74] This near-perfect elasticity makes the theory of entropic elasticity applicable,[78–80] and simplifies the analysis of the fatigue tests by excluding the inelastic effects in hydrogels of complex rheology. PAAm hydrogels are readily synthesized, and are being used in water treatment, oil recovery, agriculture, medicine,[81] as well as in most recently developed hydrogel devices.[11–15,17–19,21–26,28,29,32–35,38–40] Many of these devices directly benefit from high water content, high stretchability, nearly perfect elasticity, and transparency of PAAm. As noted above, PAAm is the primary network in many tough hydrogels.[52,55–58,60] Its property has been extensively characterized, including thermodynamics of mixing,[82,83] large deformation and swelling,[78] fracture,[52,60] adhesion with elastomers,[84] and phase seperation.[85] All these facts together make PAAm an excellent model material for fundamental studies, just as silica for studying fracture of hard materials,[86–88] and copper for studying fatigue of metals.[89–91] A comprehensive knowledge of fatigue fracture of such a model material can aid the understanding of fatigue fracture in other hydrogels.

Despite near-perfect elasticity, PAAm hydrogels do suffer fatigue fracture.[73–76] In our previous work, fatigue tests were conducted for PAAm hydrogels to support the studies of the effects of hygroscopic salts and toughheners. However, the effects of chain length and water content—two basic variables of a hydrogel of a covalent network—have not been systematically studied. This paper is devoted to the effect of water content on fatigue fracture of PAAm hydrogels. In addition to being a basic variable in hydrogels, water content plays important roles in applications, such as removing heat in fire-retarding blankets,[33] transporting ions in ionotronic devices,[11–17,19,22,26–29,34–40] dissolving drugs in drug-delivery systems,[6] and maintaining softness and biocompatibility in artificial tissues.[10,21,24]

In this study, we form the PAAm networks in all samples under the same conditions, and then modify the water content of each sample through solvent exchange. We study hydrogels of 96, 87, 78, and 69 wt% of water. We measure the crack extension under cyclic loads, and measure the fracture energy under monotonic loading. For the hydrogels of the four water contents, the fatigue thresholds are 4.3, 8.4, 20.5, and 64.5 J m^{-2}, and the fracture energies are 18.9, 71.2, 289 and 611 J m^{-2}. The measured thresholds agree well with the predictions of the Lake-Thomas model[67,73] for hydrogels of high water content, but not in the case of low water content.

2. Experimental section

2.1 Preparation of hydrogels

PAAm hydrogels with different water contents were prepared following the same process. We purchased from Sigma Aldrich the following substances: acrylamide (AAm, A8887), *N*,*N*′-methylenebis(acrylamide) (MBAA, M7279), *N*,*N*,*N*′,*N*′-tetramethylethylenediamine (TEMED, T7024), ammonium persulfate (APS, A9164), and lithium chloride (LiCl, 746460). All chemicals were received and used without further purification. AAm powders of 4.69 g were dissolved in 30 mL deionized water to form an aqueous solution. MBAA, TEMED and APS were then added in quantities of 0.0015, 0.0022 and 0.0036 times the weight of AAm in sequence. To dilute the concentration of the APS initiator, we dissolved APS into 1.2 mL deionized water before adding it to the precursor solution. The prepared pre-gel solution was degassed and injected into acrylic molds with dimensions of $120 \times 60 \times 1.5$ mm^3 and covered with an acrylic plate. The samples were then stored at room temperature for more than 18 hours for complete polymerization.

2.2 Modification of water content

The total mass of water in the precursor solution is 31.2 g. The mass of AAm in the pre-gel solution is 4.69 g. We assume all the monomers are polymerized to form the as-prepared hydrogel, and there is no water evaporation during the polymerization. As a result, the water content of the as-prepared hydrogel is calculated as 31.2/(31.2 + 4.69) = 87 wt%. The hydrogels were then modified through solvent exchange to 96, 78, and 69 wt% of water (Fig. 1a). When a hydrogel underwent solvent exchange, its weight was recorded daily (Fig. 1b). The corresponding weight of the hydrogel with 96, 78, and 69 wt% of water is 3.5, 0.59 and 0.42 times the weight of the as-prepared hydrogel.

To prepare a fully swollen hydrogel of 96 wt% of water, we soaked an as-prepared hydrogel in deionized water for 5 days until it reached equilibrium. To prepare hydrogels of 78 and

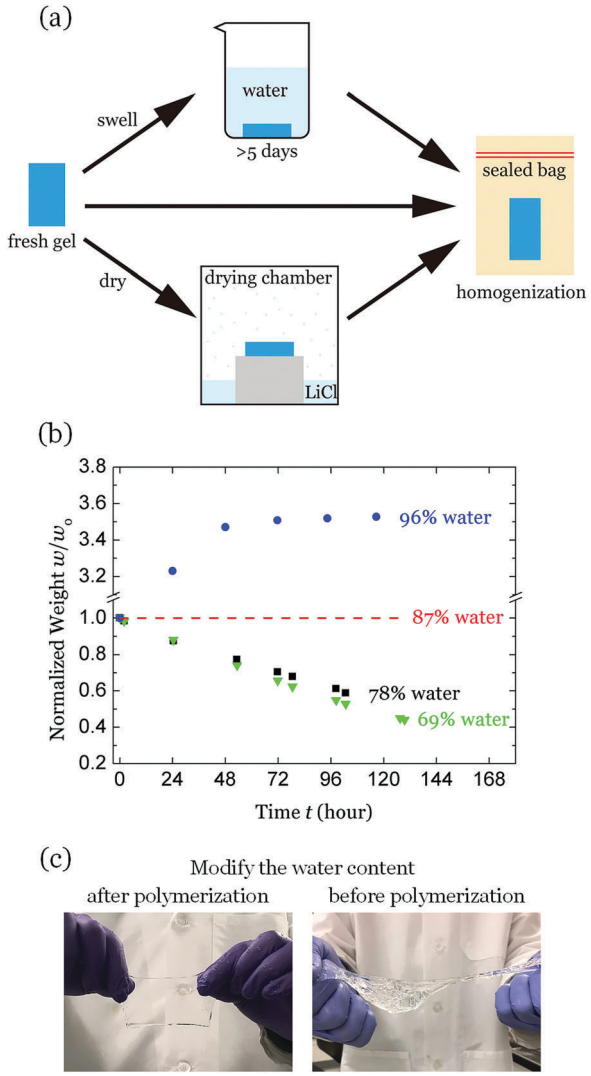

Fig. 1 Modification of the water content in PAAm hydrogels. (a) Preparation of PAAm hydrogels with a specified water content: the fully swollen hydrogels (96 wt% water) were prepared by soaking the as-prepared samples in deionized water for 5 days; the drier hydrogels (78 wt% & 69 wt%) were prepared by introducing the as-prepared samples in a chamber. After a hydrogel reached its specified water content, it was stored in a sealed bag for another 5 days to reach homogeneity. (b) The weight change of hydrogels during solvent exchange to reach specified water contents. The actual weight w is normalized by the initial weight w_0. (c) The comparison between two hydrogels of 96 wt% water made in different ways. Left: A precursor of 87 wt% water was first polymerized and then fully swollen to reach 96 wt% water. Right: A precursor of 96 wt% water was directly polymerized.

69 wt% of water, we placed an as-prepared hydrogel into a closed chamber equilibrated with 10 wt% LiCl aqueous solution (Fig. 1a). To ensure that the concentration of LiCl keeps nearly constant before and after the solvent exchange, we prepared the LiCl solution with a weight at least 100 times the weight of the hydrogel. The hydrogel was kept without direct contact with the solution, but could exchange water molecules through the moisture in the chamber. Upon reaching the expected water content after a few days, the hydrogel was taken out and sealed in a plastic bag for another 5 days for homogenization. The time scale of reaching homogenization was estimated as $t \sim L^2/D$, where L is the thickness of the hydrogel, and D is the effective diffusivity of water in the hydrogel. Taking $L \sim 10^{-3}$ m and $D \sim 10^{-10}$ m^2 s^{-1},[78] we estimated $t \sim 10^4$ s. The time period in the experiment hence ensures the homogenization of water inside the hydrogel.

Prior to solvent exchange, all samples of the hydrogels were prepared under the same condition. The PAAm network so prepared was assumed to remain unchanged after solvent exchange—that is, the water content was the only controlled variable for all samples of hydrogels. In contrast, the mechanical behavior of a hydrogel can be significantly different if its water content is varied before the formation of network (Fig. 1c). To highlight such difference, we prepared hydrogels of 96 wt% of water using two methods. In one method, we made an as-prepared hydrogel of 87 wt% of water, and then fully swelled the hydrogel in water after the polymerization (Fig. 1c left). In the other method, we added the same amount of chemical reactants, but directly prescribed 96 wt% of water in the precursor (Fig. 1c right). The two hydrogels show a significant difference in their mechanical responses. In particular, the hydrogel prepared from the precursor of 96 wt% of water is too soft and fragile to be solid-like. On the other hand, the hydrogel prepared from the precursor of 87 wt% of water and then swollen to 96 wt% of water results in a solid-like structure of the polymerized hydrogel. Such structural disparity between the hydrogels prepared in these two ways is perhaps also observed in other laboratories, but we are unable to identify any systematic study.

2.3 Setup of mechanical testing

We conducted pure shear tests to characterize the fatigue fracture of the hydrogels.[92] Before the test, we cut a piece of hydrogel and glued it with two pairs of acrylic grips using the Krazy glue. Each sample was of 70 mm width and 10 mm length between the grips. We notched the sample with a 20 mm long horizontal crack from the middle of its edge using a razor blade. The sample was then fixed in a tensile machine (Instron model 5966) with a 10 N load cell. The average thicknesses of the samples of 96, 87, 78, and 69 wt% of water were 2.35, 1.50, 1.25, and 1.10 mm.

To minimize dehydration during each test, we made an acrylic chamber to seal the tensile machine and sample (Fig. 2a). Water droplets were sprayed on the inner surface of the chamber before the test. We weighed all the samples before and after testing, and found no more than 6% weight loss. In the case of hydrogels with 96 wt% water, consider an initial hydrogel of a unit weight, of which 0.96 is water, and 0.04 is polymer. After the hydrogel loses 0.06 units of its initial weight, the water content in the hydrogel becomes $(0.96 - 0.06)/0.94 = 95.7$ wt%. Similarly, the water content of the 69 wt% hydrogel will become 67 wt% after the 6% weight loss. The maximum weight loss of 6% observed during experiments only induces slight reduction of the water content in the hydrogel, which is within the experimental error.

Fatigue fracture was tested following a cyclic linear stretch-time profile (Fig. 2b). In all tests, the stretch of the sample was

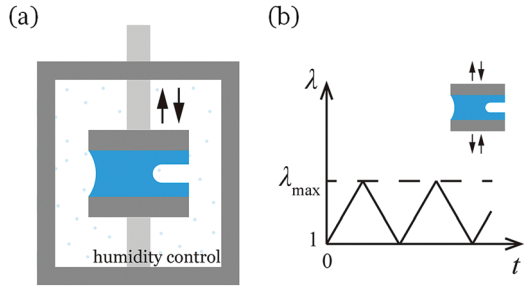

Fig. 2 Fatigue tests of hydrogels. (a) Samples were tested with a tensile machine inside a humidity chamber to prevent dehydration during the experiment. (b) The stretch-time profile of the fatigue fracture test. The stretch λ is defined as the distance between the displaced grips divided by the initial distance between the grips.

cycled between 1 and λ_{max}. We fixed the strain rate of the test to be 0.4 s^{-1}. This strain rate ensures 20 000 cycles within 8–16 hours. The effect of strain rate on fatigue is not studied in this paper. To record the crack extension, we took photos every 15 minutes (20 minutes for some tests) throughout the test with a digital camera (Canon EOS 70D). The photos were post-processed to obtain the crack extension over the loading cycles. We controlled the applied λ_{max} between 1.3 and 1.6 in all tests, so that the crack extended on the order of 0.1–1 cm in 20 000 cycles. Under the fixed strain rate of 0.4 s^{-1}, the period of one loading cycle ranged from 1.5 s to 3 s. A single fatigue fracture test typically took about 8–16 hours. The resolution of the recorded crack extension every 15 minutes was on the order of 0.1 mm.

2.4 Sharpening of the crack tip

In initial cycles, the fatigue fracture was transient, and the rate of crack extension was hardly reproducible. After some cycles, the extension of the crack reached a steady state. The similar phenomenon has been reported for elastomers.[93] In most experiments, the transient process took more than 20 000 cycles. One contributing factor to the transient process is likely that the razor blade did not prepare a consistent, sharp crack. To prepare a sharp crack, we slightly stretched the razor-notched sample by hand to let the initial crack propagate for a few millimeters before the fatigue test (Fig. 3a). We compared the fatigue crack extension of hydrogels with and without such pre-extension (Fig. 3b). With this method, the steady state was reached after ~10 000 cycles (Fig. 3c).

2.5 Quantification of the applied load

We adopted the pure shear test of Rivlin and Thomas.[92] To convert the amplitude of load to the energy release rate G, we adopted the following procedure.[60,73] We monotonically loaded an unnotched hydrogel sample of the same geometry, under a strain rate of 0.01 s^{-1} (Fig. 4a). We plotted the nominal stress (*i.e.* the applied force divided by the initial cross-sectional area) as a function of the stretch. The area under the curve gives the elastic energy per unit volume $W(\lambda)$ (Fig. 4b). The energy release rate G for a notched hydrogel under cyclic stretch of amplitude λ_{max} is

$$G = HW(\lambda_{max}), \quad (1)$$

where H is the distance of the sample between the grips in the undeformed state. We also adopted eqn (1) to quantify the *bulk toughness* of the hydrogel, with λ_{max} replaced by the critical stretch when a crack ran in a notched sample under monotonic loading. As noted before, PAAm hydrogels are nearly elastic,[73,74,77,78] the stress–stretch curve has little hysteresis, and changes negligibly over thousands of loading cycles.[74]

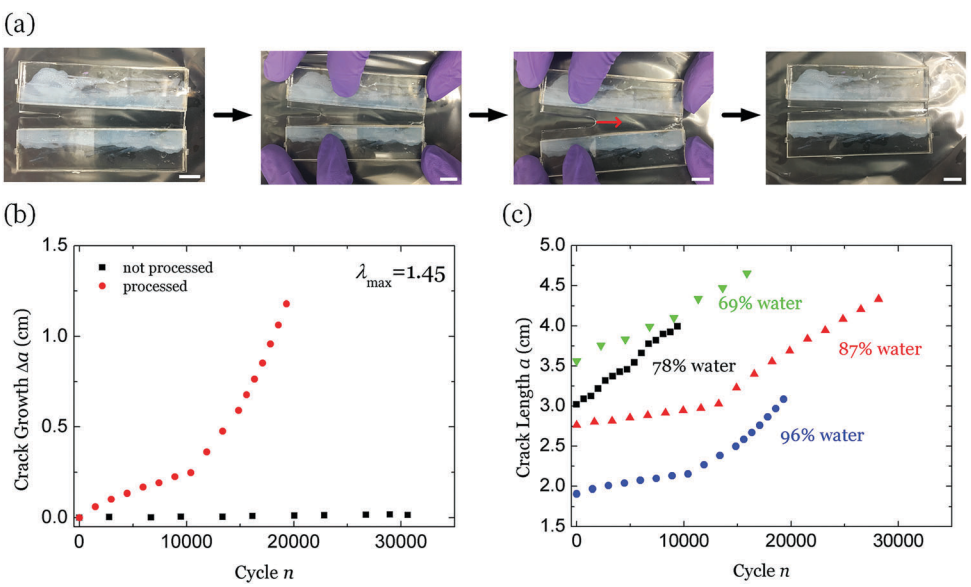

Fig. 3 Sharpening the crack tip reduces the period of transient process. (a) The crack tip initially cut by a razor blade was sharpened by slightly extending the crack before the fatigue test. The scale bar is 1 cm. (b) The fatigue crack growth of hydrogels with and without the sharpening process. (c) The representative raw experimental data of all the four hydrogels of different water content. The data typically contain transient growth, followed by steady growth.

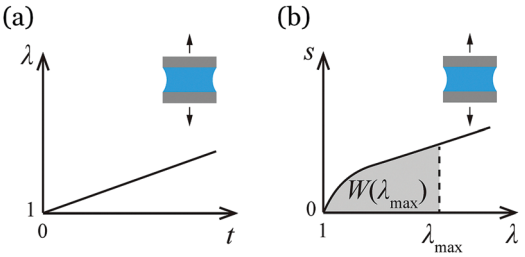

Fig. 4 Converting the applied load to the energy release rate. (a) The applied stretch as a function time. (b) The nominal stress as a function of stretch.

3. Results and discussions

In the steady state of fatigue fracture, the crack grows linearly with the number of cycles (Fig. 5a–d). We converted each applied stretch λ_{max} to the corresponding energy release rate by eqn (1) using the stress–stretch curves of unnotched hydrogels (Fig. 5e). Hydrogels with more water are more susceptible to fatigue fracture under the same level of energy release rate G. For example, at G = 8.0 J m^{-2}, a crack in the hydrogel of 96 wt% of water propagates by about 0.6 cm within 5000 cycles (Fig. 5a). In contrast, at a similar load G = 8.4 J m^{-2}, a crack in the hydrogel of 87 wt% of water only propagates less than 0.1 cm over 15 000 cycles (Fig. 5b). We recorded the crack extension of approximately 1 cm over 20 000 cycles. The mechanical loads required for such scale of crack extension per cycle are 4.0–8.0, 8.4–13.8, 19.1–34.8, and 44.4–87.0 J m^{-2}, corresponding to the hydrogels of 96, 87, 78 and 69 wt% of water, respectively.

We further compared the energy release rate for fatigue fracture in our experiments to the bulk toughness of the hydrogels. For the hydrogels of 96, 87, 78 and 69 wt% of water, the toughness was 18.9, 71.2, 289 and 611 J m^{-2}, respectively (Fig. 5f). The energy release rate for fatigue fracture is much smaller than the toughness of the hydrogel. This large difference motivates us to obtain the threshold for fatigue fracture, below which a crack does not propagate under cyclic loads.

We calculated the threshold for fatigue fracture by extrapolation of the experimental data. We performed linear regression to fit the steady-state crack growth Δa as a function of the loading cycle n. The slope of the linear curve, $\Delta a/\Delta n$, is a function of the energy release rate G (Fig. 6). $\Delta a/\Delta n$ is $\sim$50 nm per cycle when G is very small, but varies almost linearly with G when G becomes larger. The fitted linear curve intercepts the G axis at a finite value. This value, denoted as Γ_0, is the threshold for fatigue fracture. Hydrogels of fully swollen state (96 wt%) have the lowest threshold of 4.3 J m^{-2}. As the hydrogel becomes drier, the threshold increases dramatically (Fig. 6 and Table 1). Hydrogels of 69 wt% of water have a threshold of 64.5 J m^{-2}, even higher than the previously reported threshold for the PAAm–alginate tough hydrogel (53 J m^{-2}). As the water content becomes lower, the slope of $\Delta a/\Delta n$ *vs.* G decreases. That is, the crack extension in cyclic loads is slower in a drier hydrogel, compared to the same polymer network with more water. Hence, from the aspects of both the threshold and the speed of crack extension, we conclude that the resistance to fatigue fracture of a hydrogel improves when its water content is reduced.

The threshold for fatigue fracture of elastomers was described by the Lake-Thomas model as the energy required to break the covalent network and propagate the crack by unit area.[66] The Lake-Thomas model has been adapted for gels in several papers, but in different expressions.[73,94–97] Here we choose one of the adaptions, and estimate the threshold as[73]

$$\Gamma_0 = \phi_p^{2/3} bUl\sqrt{n_0}. \quad (2)$$

Here ϕ_p is the volume fraction of the polymer in the hydrogel, and is related to the water content α through

$$\phi_p = \frac{(1-\alpha)/\rho}{(1-\alpha)/\rho + \alpha/\rho_{H_2O}}, \quad (3)$$

where ρ is the density of acrylamide (1.13 g cm^{-3}), and ρ_{H_2O} is the density of water (1.0 g cm^{-3}). b is the number of C–C bonds per unit volume of the dry polymer, U is the energy of a C–C bond, l is the length of the monomer, and n_0 is the average number of monomers per chain. $bUl\sqrt{n_0}$ only depends on the PAAm network, but does not depend on the water content of the hydrogel.

For polyacrylamide, b is estimated by the number of monomers per unit volume of the dry polymer, $b = A\rho/M$ = 9.57 $\times$ 10^{27} m^{-3}, where M is the molecular weight of acrylamide (71.08 g per mole), and A is the Avogadro number (6.022 $\times$ 10^{23} per mole). The length of the monomer is estimated as $l = b^{-1/3}$ = 0.471 nm. The C–C bond energy is U = 3.3 $\times$ 10^{-19} J.[67] All together, these parameters give a value of bUl = 1.3 J m^{-2}.

The number of monomers between two crosslinks, n_0, can be estimated by $n_0 = b/N$, where N is the number of chains per unit volume of the dry polymer. Because we assume that all the hydrogels have the same PAAm network, n_0 and N are expected to be constants. To estimate N, we adopted the Gaussian chain model to the hydrogel, which relates N to the shear modulus μ through[78–80]

$$\mu = \phi_p^{1/3} NkT, \quad (4)$$

where kT is the temperature in the unit of energy. At room temperature, we take kT = 4.1 $\times$ 10^{-21} J. Experimentally, the shear modulus μ can be calculated as 1/4 of the initial slope of the stress–stretch curve under the pure shear test of unnotched samples (Fig. 5e).[73] With these, we calculated the value of N for each water content (Table 1). The calculated N varies greatly with the water content. In the current analysis, we take the average value of N = 4.4 $\times$ 10^{24} m^{-3} for all the hydrogels, and calculate the theoretical values of Γ_0 from eqn (2) accordingly.

The prediction of the Lake-Thomas model agrees well with the experimental results for hydrogels with high water content (low ϕ_p), but deviates at ϕ_p = 28%, where the experimental value of Γ_0 is much larger than the theoretical result (Fig. 7a). The same deviation occurs between the measured shear modulus μ and its theoretical prediction from the Gaussian chain model in eqn (4) (Fig. 7b). The suggested scaling of ϕ_p in eqn (2) and (4)

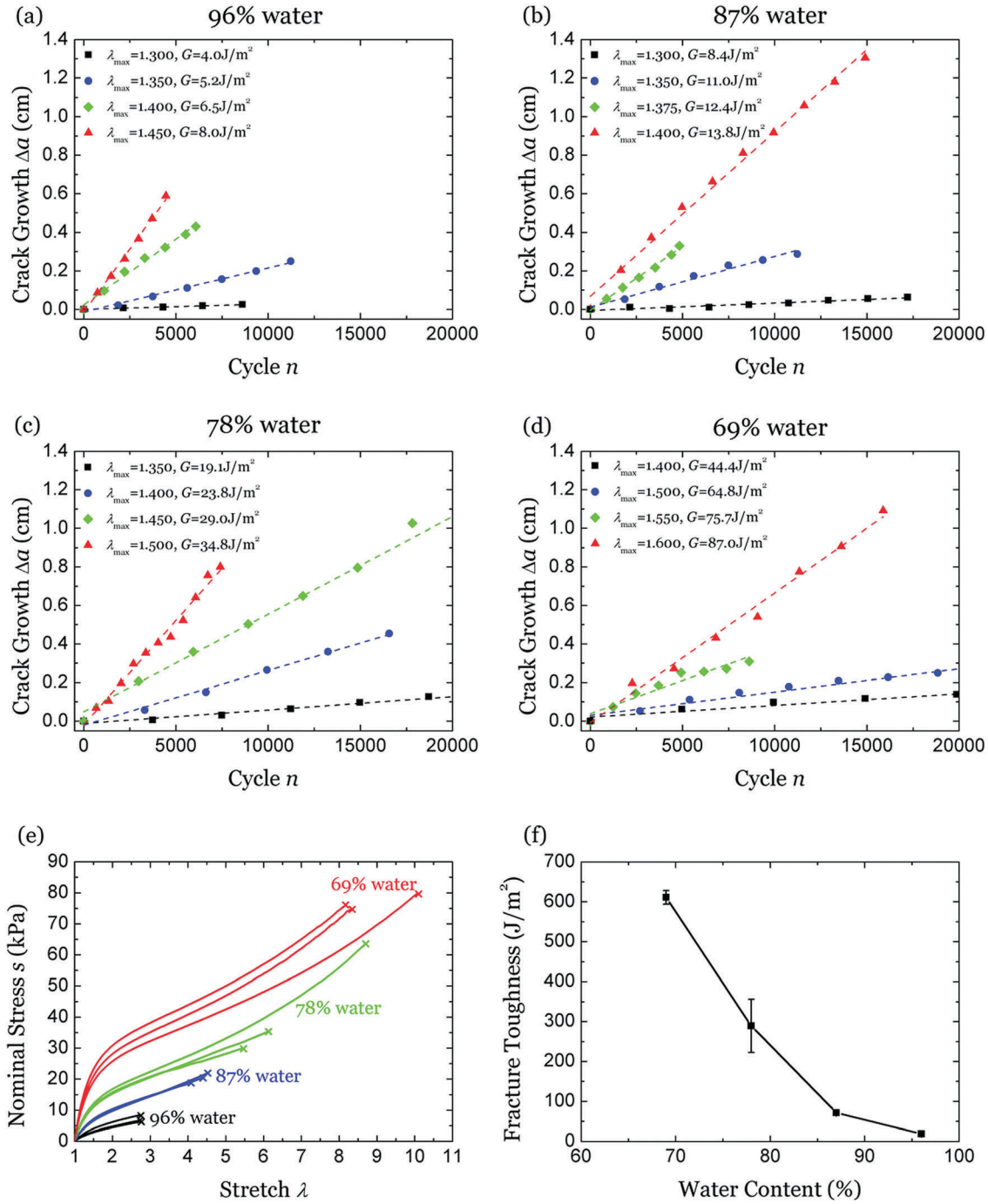

Fig. 5 Experimental data of fatigue fracture of PAAm hydrogels with different water content. The fatigue crack extension was recorded over loading cycles, in hydrogels of (a) 96 wt%, (b) 87 wt%, (c) 78 wt%, and (d) 69 wt% of water. Each curve is the representative of 3 individual tests. (e) Stress–stretch curves of unnotched hydrogels under pure shear tests. (f) The toughness decreases with the water content of the hydrogel. The data represent the mean and standard deviation of 3 experimental results.

does not fit the experimental data properly. In particular, the Lake-Thomas model adapted here does not account for the fatigue threshold of relatively dry hydrogels. Theoretical models with different scaling have been extensively studied in polymer physics,[98–100] and may shed light on resolving this discrepancy. For example, at a high polymer volume fraction ϕ_p, it is hypothesized that the presence of polymer chain entanglements may have non-trivial contribution to the threshold and shear modulus.[100] To better understand this deviation, more experimental data and improved theoretical analysis are currently under study.

Despite this deviation, both the experimental results and the Lake-Thomas model show that lower water content (or higher polymer volume fraction) enhances the threshold. In addition, the Lake-Thomas model indicates that the

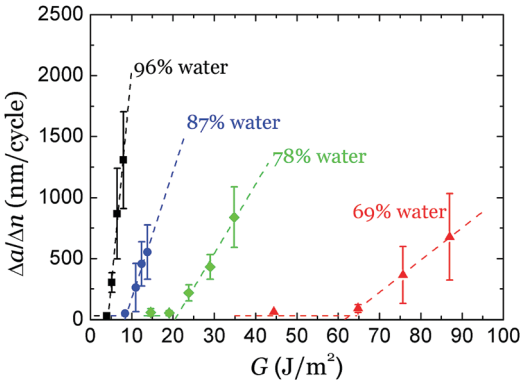

Fig. 6 The crack extension per cycle $\Delta a/\Delta n$ as a function of the energy release rate G. All the data represent the mean and standard deviation of 3 experimental results.

Table 1 Properties of PAAm hydrogels

Water content α (%)	Polymer volume fraction ϕ_p (%)	Threshold Γ_0 (J m^{-2})	Toughness (J m^{-2})	Shear modulus μ (kPa)	Chain density N (10^{24} m^{-3})
96	3.6	4.3	18.9	2.80 ± 0.32	2.07
87	12	8.4	71.2	5.92 ± 0.22	2.93
78	20	20.5	289	11.27 ± 0.46	4.70
69	28	64.5	611	21.09 ± 0.92	7.86

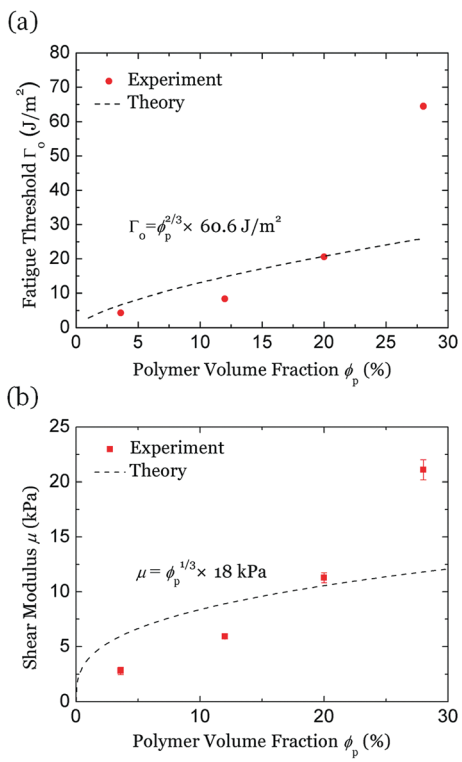

Fig. 7 Comparison between the experimental results and the theoretical prediction. (a) Fatigue threshold, theoretically predicted by the Lake-Thomas model in eqn (2). (b) Shear modulus, theoretically predicted by the Gaussian chain model in eqn (4). The four data points correspond to the hydrogels of 96, 87, 78, and 69 wt% of water, from left to right. The data in (b) represent the mean and standard deviation of 3 experimental results.

threshold increases with n_0, the average number of monomers per chain.

4. Concluding remarks

Polyacrylamide hydrogels are highly stretchable and nearly elastic. Despite this near-perfect elasticity, polyacrylamide hydrogels are susceptible to fatigue fracture. A sample without a pre-cut crack can sustain thousands of loading cycles without appreciable degradation in stress–stretch curves. When a sample with a pre-cut crack is subject to a cyclic load, however, the crack will extend cycle by cycle if the amplitude of the load (measured by energy release rate) exceeds a threshold. Here, we have characterized the effect of water content on fatigue threshold and fracture energy. Both the fatigue threshold and the fracture energy reduce as the water content increases. For hydrogels of fixed water content, the fatigue threshold is well below the fracture energy. So far as fatigue fracture is concerned, polyacrylamide hydrogels are not elastic enough. Some toughening mechanisms must exist to account for the large difference between the fatigue threshold and facture energy. For polyacrylamide hydrogels of low water content, the measured fatigue threshold is significantly higher than the prediction of the Lake-Thomas model. These findings await further study.

Conflicts of interest

There are no conflicts of interest to declare.

Acknowledgements

This work was supported by MRSEC (DMR-14-20570). E. Z. was supported by a scholarship from Tsinghua University as a visiting scholar for six months at Harvard University. X. P. M. was supported by the Cabeaux-Jacobs BAEF fellowship and by John A. Paulson School of Engineering and Applied Sciences at Harvard.

References

1 O. Wichterle and D. Lim, *Nature*, 1960, **185**, 117.
2 E. Caló and V. V. Khutoryanskiy, *Eur. Polym. J.*, 2015, **65**, 252–267.
3 F. Masuda, *Superabsorbent Polymers*, American Chemical Society, 1994, vol. 573, ch. 7, pp. 88–98.
4 K. Y. Lee and D. J. Mooney, *Chem. Rev.*, 2001, **101**, 1869–1880.
5 P. S. Lienemann, M. P. Lutolf and M. Ehrbar, *Adv. Drug Delivery Rev.*, 2012, **64**, 1078–1089.
6 J. Li and D. J. Mooney, *Nat. Rev. Mater.*, 2016, **1**, 16071.
7 J. Liu, Y. Pang, S. Zhang, C. Cleveland, X. Yin, L. Booth, J. Lin, Y. A. Lucy Lee, H. Mazdiyasni, S. Saxton, A. R. Kirtane, T. V. Erlach, J. Rogner, R. Langer and G. Traverso, *Nat. Commun.*, 2017, **8**, 124.

8 J. Li, A. D. Celiz, J. Yang, Q. Yang, I. Wamala, W. Whyte, B. R. Seo, N. V. Vasilyev, J. J. Vlassak, Z. Suo and D. J. Mooney, *Science*, 2017, **357**, 378–381.

9 M. A. Haque, T. Kurokawa and J. P. Gong, *Polymer*, 2012, **53**, 1805–1822.

10 L. Xu, X. Zhao, C. Xu and N. A. Kotov, *Adv. Mater.*, 2018, **30**, 1703343.

11 C. Keplinger, J. Y. Sun, C. C. Foo, P. Rothemund, G. M. Whitesides and Z. Suo, *Science*, 2013, **341**, 984–987.

12 E. Acome, S. Mitchell, T. Morrissey, M. Emmett, C. Benjamin, M. King, M. Radakovitz and C. Keplinger, *Science*, 2018, **359**, 61–65.

13 N. Kellaris, V. G. Venkata, G. M. Smith, S. K. Mitchell and C. Keplinger, *Science*, 2018, **3**, eaar3276.

14 Y. Bai, Y. Jiang, B. Chen, C. Chiang Foo, Y. Zhou, F. Xiang, J. Zhou, H. Wang and Z. Suo, *Appl. Phys. Lett.*, 2014, **104**, 062902.

15 B. Chen, Y. Bai, F. Xiang, J. Y. Sun, Y. Mei Chen, H. Wang, J. Zhou and Z. Suo, *J. Polym. Sci., Part B: Polym. Phys.*, 2014, **52**, 1055–1060.

16 C. Xu, B. Li, C. Xu and J. Zheng, *J. Mater. Sci.: Mater. Electron.*, 2015, **26**, 9213–9218.

17 C. Zhang, W. Sun, H. Chen, L. Liu, B. Li and D. Li, *J. Appl. Phys.*, 2016, **119**, 094108.

18 H. Yuk, S. Lin, C. Ma, M. Takaffoli, N. X. Fang and X. Zhao, *Nat. Commun.*, 2017, **8**, 14230.

19 T. Li, G. Li, Y. Liang, T. Cheng, J. Dai, X. Yang, B. Liu, Z. Zeng, Z. Huang and Y. Luo, *Sci. Adv.*, 2017, **3**, e1602045.

20 G. Haghiashtiani, E. Habtour, S.-H. Park, F. Gardea and M. C. McAlpine, *Extreme Mech. Lett.*, 2018, **21**, 1–8.

21 S. Lin, H. Yuk, T. Zhang, G. A. Parada, H. Koo, C. Yu and X. Zhao, *Adv. Mater.*, 2016, **28**, 4497–4505.

22 J. Y. Sun, C. Keplinger, G. M. Whitesides and Z. Suo, *Adv. Mater.*, 2014, **26**, 7608–7614.

23 S. S. Robinson, K. W. O'Brien, H. Zhao, B. N. Peele, C. M. Larson, B. C. Mac Murray, I. M. Van Meerbeek, S. N. Dunham and R. F. Shepherd, *Extreme Mech. Lett.*, 2015, **5**, 47–53.

24 D. Wirthl, R. Pichler, M. Drack, G. Kettlguber, R. Moser, R. Gerstmayr, F. Hartmann, E. Bradt, R. Kaltseis, C. M. Siket, S. E. Schausberger, S. Hild, S. Bauer and M. Kaltenbrunner, *Sci. Adv.*, 2017, **3**, e1700053.

25 H. Yuk, T. Zhang, G. A. Parada, X. Liu and X. Zhao, *Nat. Commun.*, 2016, **7**, 12028.

26 M. S. Sarwar, Y. Dobashi, C. Preston, J. K. Wyss, S. Mirabbasi and J. D. W. Madden, *Sci. Adv.*, 2017, **3**, e1602200.

27 Z. Lei, Q. Wang, S. Sun, W. Zhu and P. Wu, *Adv. Mater.*, 2017, **29**, 1700321.

28 C. H. Yang, B. Chen, J. J. Lu, J. H. Yang, J. Zhou, Y. M. Chen and Z. Suo, *Extreme Mech. Lett.*, 2015, **3**, 59–65.

29 T. B. Schroeder, A. Guha, A. Lamoureux, G. VanRenterghem, D. Sept, M. Shtein, J. Yang and M. Mayer, *Nature*, 2017, **552**, 214.

30 M. Choi, M. Humar, S. Kim and S. H. Yun, *Adv. Mater.*, 2015, **27**, 4081–4086.

31 M. B. Applegate, G. Perotto, D. L. Kaplan and F. G. Omenetto, *Biomed. Opt. Express*, 2015, **6**, 4221–4227.

32 J. Guo, X. Liu, N. Jiang, A. K. Yetisen, H. Yuk, C. Yang, A. Khademhosseini, X. Zhao and S. H. Yun, *Adv. Mater.*, 2016, **28**, 10244–10249.

33 W. R. Illeperuma, P. Rothemund, Z. Suo and J. J. Vlassak, *ACS Appl. Mater. Interfaces*, 2016, **8**, 2071–2077.

34 C. C. Kim, H. H. Lee, K. H. Oh and J. Y. Sun, *Science*, 2016, **353**, 682–687.

35 X. Pu, M. Liu, X. Chen, J. Sun, C. Du, Y. Zhang, J. Zhai, W. Hu and Z. L. Wang, *Sci. Adv.*, 2017, **3**, e1700015.

36 K. Parida, V. Kumar, W. Jiangxin, V. Bhavanasi, R. Bendi and P. S. Lee, *Adv. Mater.*, 2017, **29**, 1702181.

37 W. Xu, L. B. Huang, M. C. Wong, L. Chen, G. Bai and J. Hao, *Adv. Energy Mater.*, 2017, **7**, 1601529.

38 C. H. Yang, S. Zhou, S. Shian, D. R. Clarke and Z. Suo, *Mater. Horiz.*, 2017, **4**, 1102–1109.

39 C. H. Yang, B. Chen, J. Zhou, Y. M. Chen and Z. Suo, *Adv. Mater.*, 2016, **28**, 4480–4484.

40 C. Larson, B. Peele, S. Li, S. Robinson, M. Totaro, L. Beccai, B. Mazzolai and R. Shepherd, *Science*, 2016, **351**, 1071–1074.

41 Y. Bai, B. Chen, F. Xiang, J. Zhou, H. Wang and Z. Suo, *Appl. Phys. Lett.*, 2014, **105**, 151903.

42 P. Le Floch, X. Yao, Q. Liu, Z. Wang, G. Nian, Y. Sun, L. Jia and Z. Suo, *ACS Appl. Mater. Interfaces*, 2017, **9**, 25542–25552.

43 Q. Liu, G. Nian, C. Yang, S. Qu and Z. Suo, *Nat. Commun.*, 2018, **9**, 846.

44 A. Agrawal, N. Rahbar and P. D. Calvert, *Acta Biomater.*, 2013, **9**, 5313–5318.

45 I. Liao, F. T. Moutos, B. T. Estes, X. Zhao and F. Guilak, *Adv. Funct. Mater.*, 2013, **23**, 5833–5839.

46 W. R. Illeperuma, J.-Y. Sun, Z. Suo and J. J. Vlassak, *Extreme Mech. Lett.*, 2014, **1**, 90–96.

47 M. T. I. Mredha, Y. Z. Guo, T. Nonoyama, T. Nakajima, T. Kurokawa and J. P. Gong, *Adv. Mater.*, 2018, **30**, 1704937.

48 H. Yuk, T. Zhang, S. Lin, G. A. Parada and X. Zhao, *Nat. Mater.*, 2016, **15**, 190–196.

49 K. Tian, J. Bae, S. E. Bakarich, C. Yang, R. D. Gately, G. M. Spinks, M. i. h. Panhuis, Z. Suo and J. J. Vlassak, *Adv. Mater.*, 2017, **29**, 1604827.

50 S. Hong, D. Sycks, H. F. Chan, S. Lin, G. P. Lopez, F. Guilak, K. W. Leong and X. Zhao, *Adv. Mater.*, 2015, **27**, 4035–4040.

51 A. S. Gladman, E. A. Matsumoto, R. G. Nuzzo, L. Mahadevan and J. A. Lewis, *Nat. Mater.*, 2016, **15**, 413.

52 J. P. Gong, Y. Katsuyama, T. Kurokawa and Y. Osada, *Adv. Mater.*, 2003, **15**, 1155–1158.

53 C. Chen, Z. Wang and Z. Suo, *Extreme Mech. Lett.*, 2017, **10**, 50–57.

54 X. Zhao, *Proc. Natl. Acad. Sci. U. S. A.*, 2017, **114**, 8138–8140.

55 J. P. Gong, *Soft Matter*, 2010, **6**, 2583–2590.

56 M. A. Haque, T. Kurokawa and J. P. Gong, *Soft Matter*, 2012, **8**, 8008–8016.

57 J. Li, Z. Suo and J. J. Vlassak, *J. Mater. Chem. B*, 2014, **2**, 6708–6713.

58 Y. Yang, X. Wang, F. Yang, H. Shen and D. Wu, *Adv. Mater.*, 2016, **28**, 7178–7184.

59 X. Zhao, *Soft Matter*, 2014, **10**, 672–687.

60 J. Y. Sun, X. Zhao, W. R. Illeperuma, O. Chaudhuri, K. H. Oh, D. J. Mooney, J. J. Vlassak and Z. Suo, *Nature*, 2012, **489**, 133–136.
61 C. Creton, *Macromolecules*, 2017, **50**, 8297–8316.
62 W. Wang, Y. Zhang and W. Liu, *Prog. Polym. Sci.*, 2017, **71**, 1–25.
63 Y. S. Zhang and A. Khademhosseini, *Science*, 2017, **356**, eaaf3627.
64 P. C. Paris, M. P. Gomez and W. E. Anderson, *Trend Eng.*, 1961, **13**, 9–14.
65 A. Thomas, *J. Polym. Sci.*, 1958, **31**, 467–480.
66 G. Lake and P. Lindley, *J. Appl. Polym. Sci.*, 1965, **9**, 1233–1251.
67 G. Lake and A. Thomas, *Proc. R. Soc. London, Ser. A*, 1967, **300**, 108–119.
68 G. Lake, *Rubber Chem. Technol.*, 1995, **68**, 435–460.
69 W. Mars and A. Fatemi, *Rubber Chem. Technol.*, 2004, **77**, 391–412.
70 A. N. Gent, *Engineering with rubber: how to design rubber components*, Carl Hanser Verlag GmbH Co KG, 2012.
71 R. Ritchie, *Mater. Sci. Eng., A*, 1988, **103**, 15–28.
72 S. Suresh, *Fatigue of materials*, Cambridge university press, 1998.
73 J. Tang, J. Li, J. J. Vlassak and Z. Suo, *Extreme Mech. Lett.*, 2017, **10**, 24–31.
74 R. Bai, Q. Yang, J. Tang, X. P. Morelle, J. Vlassak and Z. Suo, *Extreme Mech. Lett.*, 2017, **15**, 91–96.
75 W. Zhang, X. Liu, J. Wang, J. Tang, J. Hu, T. Lu and Z. Suo, *Eng. Fract. Mech.*, 2018, **187**, 74–93.
76 R. Bai, J. Yang, X. P. Morelle, C. Yang and Z. Suo, *ACS Macro Lett.*, 2018, 312–317, DOI: 10.1021/acsmacrolett.8b00045.
77 J. Zhang, C. R. Daubert and E. A. Foegeding, *Rheol. Acta*, 2005, **44**, 622–630.
78 J. Li, Y. Hu, J. J. Vlassak and Z. Suo, *Soft Matter*, 2012, **8**, 8121–8128.
79 W. Hong, X. Zhao, J. Zhou and Z. Suo, *J. Mech. Phys. Solids*, 2008, **56**, 1779–1793.
80 S. Cai and Z. Suo, *EPL*, 2012, **97**, 34009.
81 M. J. Caulfield, G. G. Qiao and D. H. Solomon, *Chem. Rev.*, 2002, **102**, 3067–3084.
82 A. Hochberg, T. Tanaka and D. Nicoli, *Phys. Rev. Lett.*, 1979, **43**, 217.
83 J. C. Day and I. D. Robb, *Polymer*, 1981, **22**, 1530–1533.
84 J. Tang, J. Li, J. J. Vlassak and Z. Suo, *Soft Matter*, 2016, **12**, 1093–1099.
85 K. Sato, T. Nakajima, T. Hisamatsu, T. Nonoyama, T. Kurokawa and J. P. Gong, *Adv. Mater.*, 2015, **27**, 6990–6998.
86 A. A. Griffith and M. Eng, *Philos. Trans. R. Soc. London, Ser. A*, 1921, **221**, 163–198.
87 E. Orowan, *Nature*, 1944, **154**, 341.
88 S. Wiederhorn and L. Bolz, *J. Am. Ceram. Soc.*, 1970, **53**, 543–548.
89 N. Thompson, N. Wadsworth and N. Louat, *Philos. Mag.*, 1956, **1**, 113–126.
90 K. Katagiri, A. Omura, K. Koyanagi, J. Awatani, T. Shiraishi and H. Kaneshiro, *Metall. Trans. A*, 1977, **8**, 1769–1773.
91 Z. Basinski, A. Korbel and S. Basinski, *Acta Metall.*, 1980, **28**, 191–207.
92 R. Rivlin and A. Thomas, *J. Polym. Sci.*, 1953, **10**, 291–318.
93 S. Mzabi, D. Berghezan, S. Roux, F. Hild and C. Creton, *J. Polym. Sci., Part B: Polym. Phys.*, 2011, **49**, 1518–1524.
94 C. Creton and M. Ciccotti, *Rep. Prog. Phys.*, 2016, **79**, 046601.
95 H. Mueller and W. Knauss, *Trans. Soc. Rheol.*, 1971, **15**, 217–233.
96 A. Ahagon and A. Gent, *J. Polym. Sci., Part B: Polym. Phys.*, 1975, **13**, 1903–1911.
97 Y. Akagi, H. Sakurai, J. P. Gong, U.-I. Chung and T. Sakai, *J. Chem. Phys.*, 2013, **139**, 144905.
98 P.-G. De Gennes, *Scaling concepts in polymer physics*, Cornell university press, 1979.
99 S. P. Obukhov, M. Rubinstein and R. H. Colby, *Macromolecules*, 1994, **27**, 3191–3198.
100 M. Rubinstein and R. H. Colby, *Polymer Physics*, Oxford University Press, New York, 2003.